

Development of an ISO8729 compliant passive RCS enhancer, part 2.

- design of metallic waveguide lenses -

Derek GRAY and Julien Le KERNEC

James Watt School of Engineering, University of Glasgow, Glasgow, UK.

E-mail: (Derek.Gray, Julien.LeKervec) @glasgow.ac.uk

Abstract An aplanatic lens backed by an offset conductive bowl was found to satisfy the ISO8729 passive RCS enhancer recommendation in a 12GHz scaled model across $\pm 25^\circ$. Four wavelength radius, negative refractive index lenses composed of air or foam filled hexagonal waveguide were investigated as potential low mass and low cost alternatives to the natural plastic aplanatic lenses used in the past. The focal arc angular spread and position were studied in simulation at 9.41GHz for $f/D=0.3$ to $f/D=1$, and were found to be equivalent to the focusing ability of the prior natural plastic lenses. The maximum lens thickness was less than $1.5\lambda_0$.

Key words lens antenna, RCS enhancer.

1. Introduction

Fishing boats, yachts and other small marine vessels under 150 gross tonnage (GT) are poor reflectors of radar signals as these sit low in the water and the hulls are either low reflectivity glass fibre reinforced plastic (FRP) or wood. This lack of radar detectability contributes to the 2 or so small vessel collisions per day in Japanese green waters. Without a legal compulsion for small vessels to at least carry ISO8729 compliant passive RCS enhancers, the only alternative is to reduce the cost to a point where there is no economic disincentive to the adoption of those. As a follow on to a programme at Tokyo University of Marine Science and Technology, a range of potentially low cost passive RCS enhancers were studied as 12GHz scaled models [1]. A double convex aplanatic lens cut to a square fitted with a reflective bowl worked across $\pm 25^\circ$, so a set of 5 would satisfy the ISO8729 horizon coverage recommendation [2]. These would presumably be suspended in a foam matrix attached to the mast top. Here the design of the aplanatic lens is

examined with some care at the actual operating frequency of 9.41GHz. The design of natural plastic aplanatic 9.41GHz lenses was considered in [3] with an $f/D=0.4$ lens giving a satisfactory flat focal arc across scan angles of 0° to 30° .

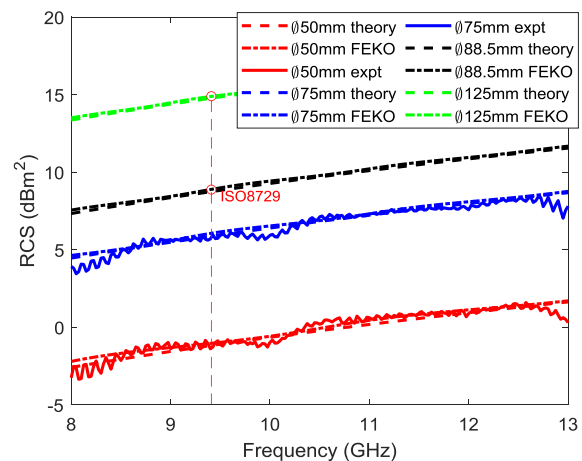


Figure 1: Theoretical, simulated & measured on axis RCS of flat 1mm thick aluminium disks.

The ISO8729 recommendation for passive RCS enhancers specifies an RCS of 7.75dBm² at 9.41GHz [2]. This is the RCS of a 88.5mm radius flat disk, Figure 1. Adding 6dB as a margin would require the disk radius be

increased to 125mm ($4\lambda_0$), which was used as the aperture size for this work on aplanatic lenses.

The design procedure and measured results for the first successful radio frequency aplanatic $n>1$ lens were published in 1889 [4]. Foundational work on both $n>1$ and $n<1$ lenses was done during WW2 when there was a need for medium to high Gain X-band radar antennas. Self-supporting metallic mesh or honeycomb $n<1$ lenses are of interest as are presumed to be lower mass and be more durable as will not be damaged by UV light. Likewise, a metal foil honeycomb lens inside the foam matrix of a float or buoy will add little to the mass of the foam. The aim of this work was to prepare a library of $n<1$ lenses for which the $\pm 45^\circ$ focal arc is as close to lens as possible that will be fitted with customized reflective bowls in future work.

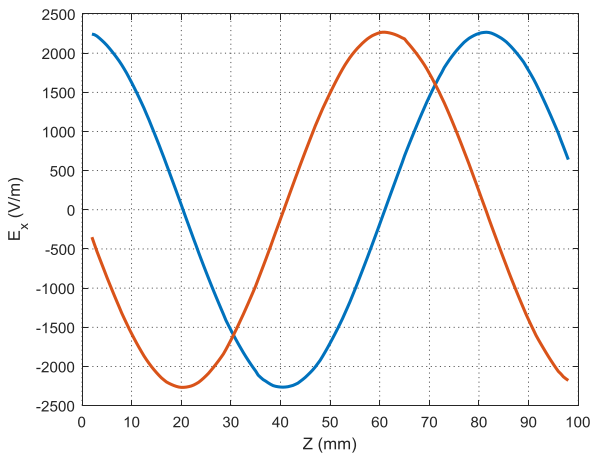


Figure 2: E-field along centre-line of an 11mm radius hexagonal cross-section waveguide at 9.41GHz; from FEKO™ (FEM solver).

Metallic honeycombs are used extensively in aerospace structures as have higher strength than square or rectangular tessellations. It is understood that metallic tubing of arbitrary cross-section can be used as waveguides [5-7], although a numerical simulator need be used to determine the guided wavelength (λ_g) and other electrical properties as there are no closed form empirical equations. A 100mm long section of 11mm radius hexagonal cross-section waveguide terminated in an absorbing load was simulated in the Finite Element Method (FEM) solver in FEKO™ at 9.41GHz and the

E-field along its axis extracted. The half guided wavelength ($\lambda_g/2$) was found to be 41mm, Figure 2; been equivalent to a 10.1mm radius circular waveguide. The 125mm radius target aperture was populated with 11mm radius hexagons which with spillover gave a base structure fitting inside a 315mm radius, Figure 3.

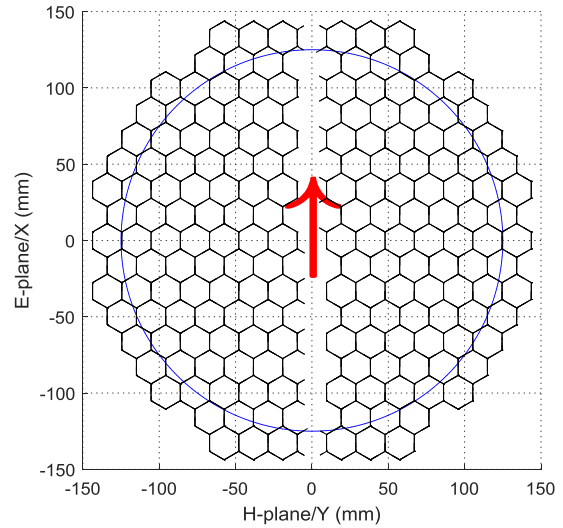


Figure 3: Base honeycomb structure definition with E-field direction & 125mm aperture marked.

The marine passive RCS enhancer application is simple in that it is horizontally polarized and as the lenses are rotationally symmetric it only required scanning in the plane of the E-field vector in FEKO™ MoM simulation, as indicated in Figure 3. The Electric near field was calculated for $z=-50$ to 250mm as a fixed standard for all lenses, then processed in Matlab™. The natural plastic lenses focused to a cigar shaped region and not a point as were electrically small at $4\lambda_0$ radius [3]. The FEKO™ models were run for plane wave incident angles of 0° to 45° in 5° steps, the electric near field was retained and processed to find the peak positions which were then plotted as the focal arc. The same was done here for the honeycomb lenses but as some were thin those could also be simulated in the FEM solver and the calculated E-field data processed in the same manner then been directly comparable to the MoM simulation results, Figures 4 and 5. This was done for both standard and fine meshing. The pairs of MoM and FEM results were near identical and there was reasonable agreement between the 2 types

for both focal region position and amplitude giving a high degree of confidence in the MoM results throughout.

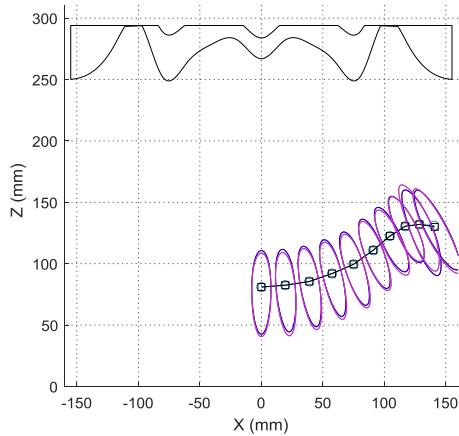


Figure 4: Scanning performance comparison of FEM and MoM simulations of a foam supported thin lens; trace colours as per Figure 5, lens profile between Z=250mm and Z=300mm, from FEKO™.

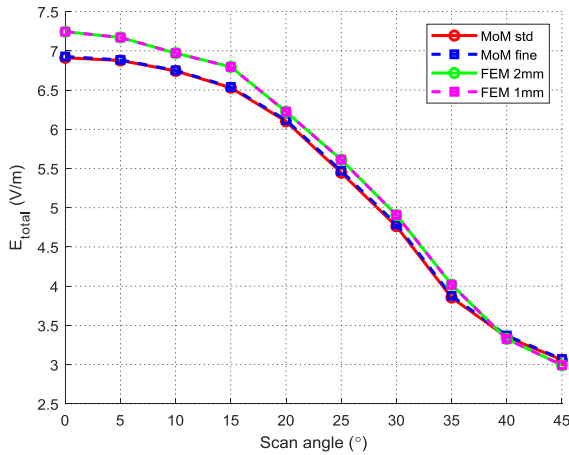


Figure 5: Focal arc E-field strength variation with scan angle comparison of FEM and MoM simulations of a foam supported thin lens; from FEKO™.

A 2 diffracting surface plano-convex lens design was generated for 125mm radius and $\epsilon_r=2.3$ with a 5mm edge using the equation in Figure 18-2 of [8], been used as a baseline lens design here as it was in [3] as “b.line.”

A multitude of $n<1$ lens variants are described in [8]. Each of the general type were investigated here.

2. Concave-plano lens

The simplest type of $n<1$ lens has a flat upper surface which made the lower surface an ellipse [8]. Having one flat face simplifies lay-up if assembling from sections of air or foam filled tubing. The Genetic Algorithm (GA)

optimizer was used in [3] to find novel $n>1$ lens designs. Here the upper surface was kept flat and the lower surface was a rotationally symmetric Non Uniform Rational B-Spline (NURBS) in FEKO™, Figure 6. The GA was run until an E-field greater than 6V/m was obtained at some target focal position. This was successful for $f/D=0.55$ down to 0.45, which appears to be a physical limit, Figure 7; shorter f/D could not be achieved.

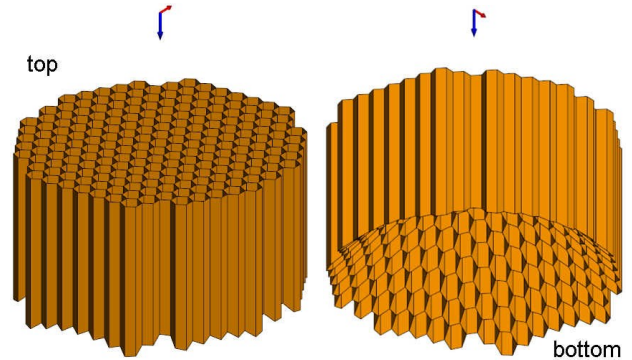


Figure 6: CAD of concave-plano lens GA #1; from FEKO™.

The focal arc of GA #1 was flat at $f/D=0.5$ to a scan angle of 20°, inferring that the reflective bowl could be a saucepan shape, Figure 7.

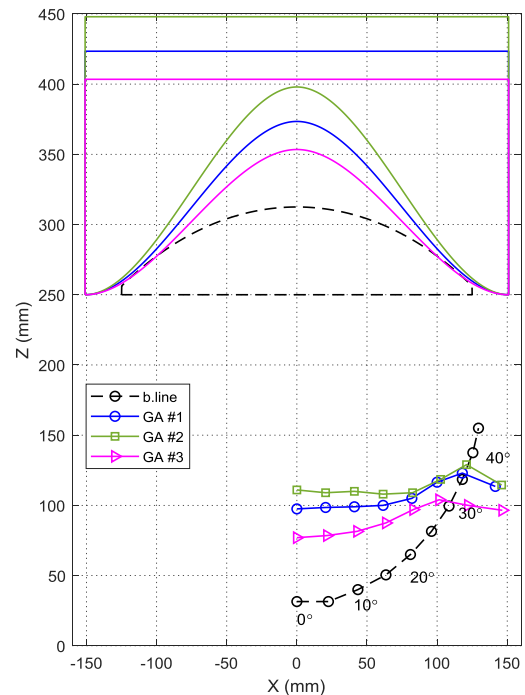


Figure 7: Electric near field for scan angles 0° to 45° of concave-plano lenses; lens profiles same colours as focal arcs, from FEKO™.

The concave surface was 51mm deep for all 3 cases, while the total honeycomb length was 150 to 200mm.

3. Spherical-concave lenses

The majority of deployed square metallic waveguide lenses have had a spherical lower concave face while the upper concave surface was designed to match, and zoned to minimize mass. A series with spherical lower faces was run in FEKO™, with the radius r fixed between the lens lower rim and the target focal point, Figure 8.

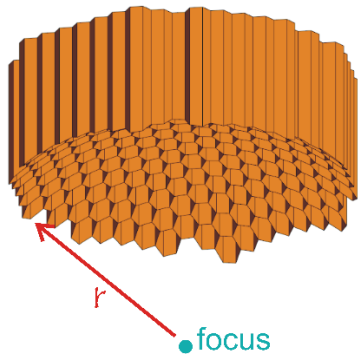


Figure 8: CAD of spherical-concave lens; from FEKO™.

As the f/D was decreased from 0.7 to 0.43, the focal arc flattened, Figure 9. However, as for the concave-plano type above $f/D \approx 0.43$ appeared to be a physical limit as no shorter f/D were achieved.

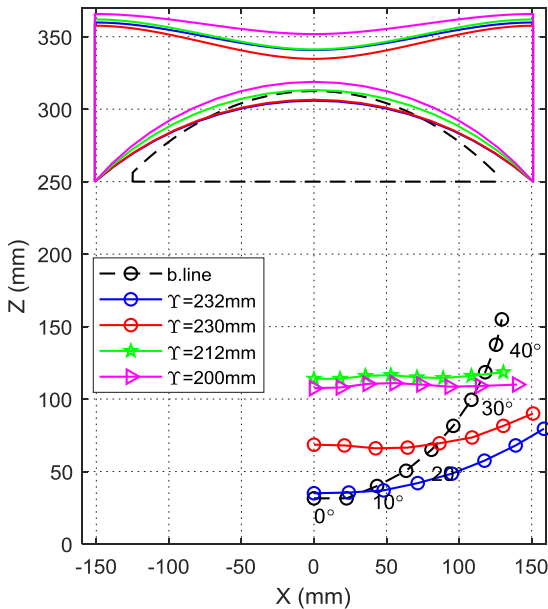


Figure 9: Electric near field for scan angles 0° to 45° of spherical-concave lenses; lens profiles same colours as focal arcs, from FEKO™.

Comparing Figures 7 and 9, for the limiting $f/D \approx 0.45$ cases, the spherical lower surface types had flatter focal arcs to 45° which is a distinct advantage, as was the overall lens length reducing to 110mm.

4. Genetic algorithm double concave lenses

The lower surface of the FEKO™ model was changed to a GA controlled rotational NURBS with a constraint that there must always be greater than 5mm between it and the upper surface GA controlled NURBS. The f/D was successfully decreased from 0.55 to 0.35 in 0.05 steps with all 4 designs giving relatively flat focal arcs to 35° scan angle, Figure 10.

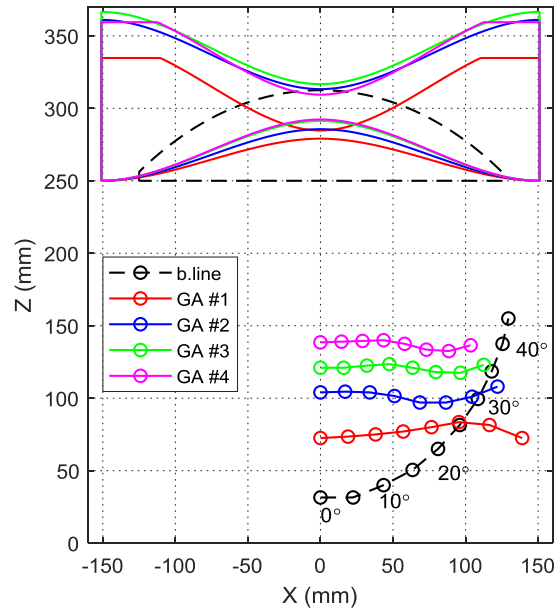


Figure 10: Electric near field for scan angles 0° to 45° of double concave lenses; lens profiles same colours as focal arcs, from FEKO™.

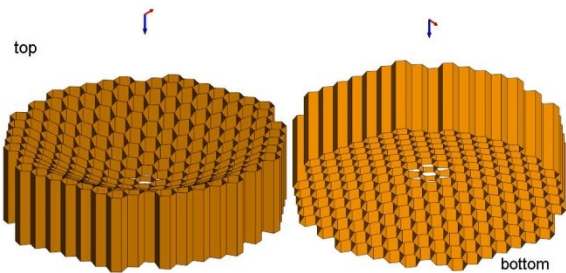


Figure 11: CAD of GA #1; from FEKO™.

Design GA #1 was relatively short at 85mm been thinnest at the centre with 6.5mm thickness, Figure 11. Built from marine grade aluminium alloy shim, this lens would likely be robust enough to not require a radome. The other 3 designs were all about 110mm long with centres from 20 to 30mm thick, which should survive long term exposure to the marine environment.

As GA #1 was about $1\lambda_g$ long and the other 3 about $1.5\lambda_g$

long, there was some suspicion that these lenses were resonating as opposed to being pure travelling wave devices as is usually supposed. A 2D E-field slice through the centre of GA #1 showed low field strength at the lens centre and a confusing checkerboard pattern at the edge, Figure 13. Importing the near field data into Matlab™ and plotting 3V/m contours (been about half the peak focal zone amplitude) showed that the 2 outer lines of waveguide supported 2 standing wave peaks at high amplitude, Figure 13. This is not unexpected as those sections of waveguide are all $\approx 1\lambda_g$ in length. At half the lens radius there were 2 concentric rings supporting a single but lower intensity resonance, which in turn is not unexpected as those sections of waveguide are all $\approx \lambda_g/2$ in length. Thus it has been found that this class of $n < 1$ lenses support significant resonances and are not pure travelling wave antennas.

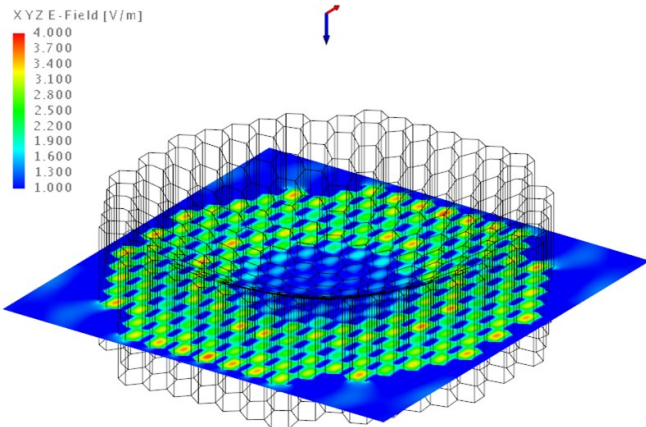


Figure 12: 2D Electric near field slice through the $f/D=0.55$ GA #1 lens for scan angle 0° ; from FEKO™.

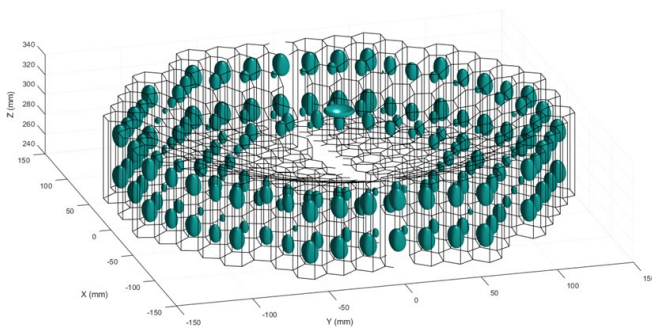


Figure 13: 3V/m 3D electric near field in the $f/D=0.55$ GA #1 lens for scan angle 0° ; same data as Figure 10, from FEKO™.

5. Genetic algorithm foam supported thin lenses

The FEKO™ model was further modified to allow the upper and lower GA controlled rotational NURBS to cross, which would break the structure and require foam or aerogel supports but minimize the overall lens thickness. The GA was run until an E-field greater than 6V/m was obtained at some target focal position, as before. Successful scanning $f/D=0.55$ to $f/D=0.3$ lens designs were obtained, Figure 14.

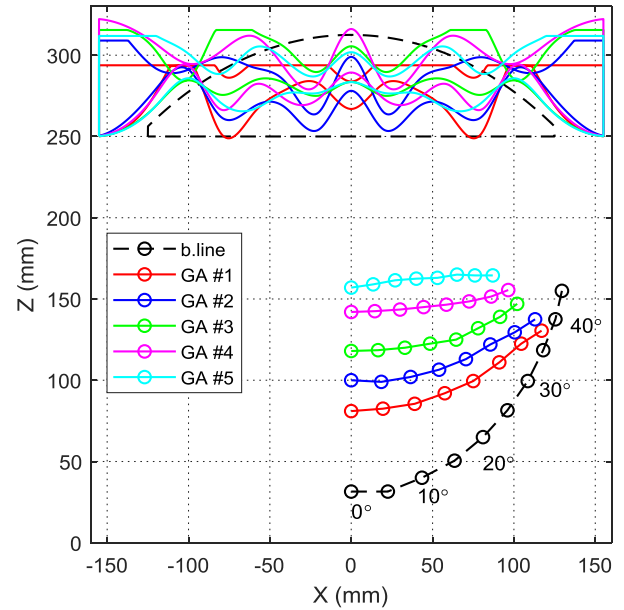


Figure 14: Electric near field for scan angles 0° to 45° of foam supported lenses; lens profiles same colours as focal arcs, from FEKO™.

The edge thickness of GA #1 was 44mm while GA #4 was 72mm. Thus none of the 5 designs had any dimension greater than λ_g . Design GA #1, as an example, had a flat upper surface except for the small concave inclusion on its axis, Figure 15. Consequently this design can conveniently be affixed to and assembled on a simple flat foam or aerogel support, as could all the others except GA #4.

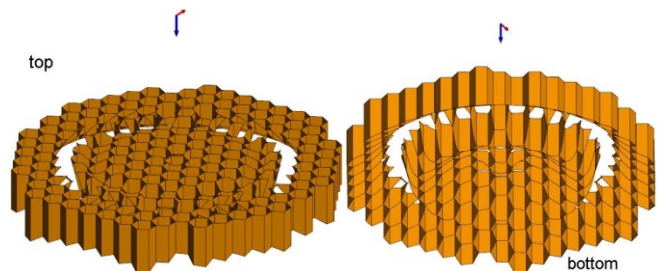


Figure 15: CAD of GA #1; from FEKO™.

The focal zone peak E-field intensity from 0° scan for lens GA # 1 was 7V/m in MoM simulation and 7.25V/m from FEM, Figure 5. Slicing through the centre of GA #1, the E-field peaks were 3.5V/m been about half of the focal zone peak, Figure 16. In contrast to Figure 12, there were distinct concentric rings of high E-field strength but identification of standing waves was not possible from the 2D slice plots. Whereas plotting the 3V/m 3D contour clearly showed those, Figure 17. The number of waveguide sections supporting standing waves was significantly reduced compared to the double concave above, Figures 13 and 17. The intensity or volume occupied by the peaks was also reduced. This lens is thus closer to the ideal optical principal.

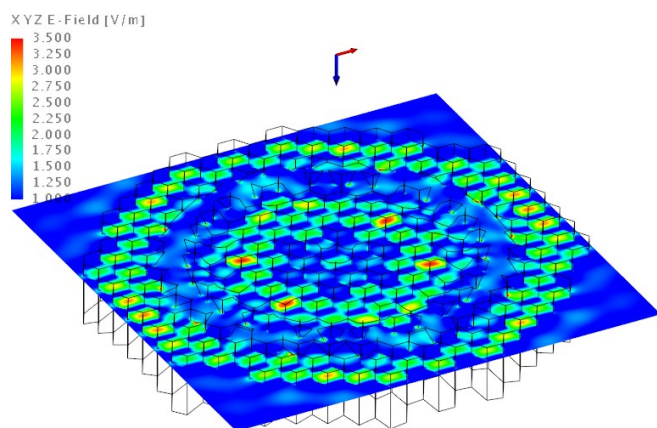


Figure 16: 2D Electric near field slice through the $f/D=0.4$ GA #1 lens for scan angle 0° ; from FEKO™.

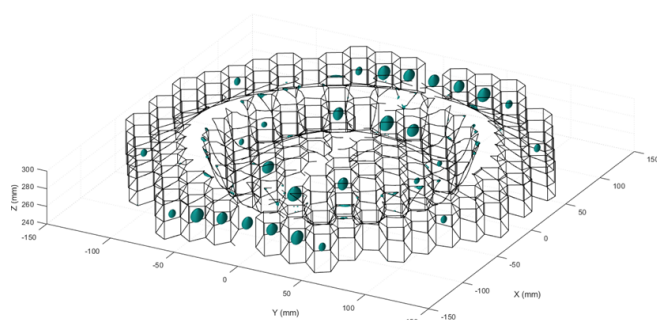


Figure 17: 3V/m 3D electric near field in the $f/D=0.4$ GA #1 lens for scan angle 0° ; same data as Figure 14, from FEKO™.

6. Conclusions

A series of $n < 1$ aplanatic lenses formed from metallic

honeycomb were investigated to find types that had focal arcs for $\pm 45^\circ$ scanning close to the lens for a marine passive RCS enhancer application. Good performance scan performance for $f/D=0.55$ to $f/D=0.35$ was found for a GA modified concave-concave lenses. Standing waves were found in all of the lenses examined. Thinning the lenses to the point of blanking minimized the amplitude of the standing waves. The effects of these resonances on both radiation and ohmic losses will be examined in future work.

7. References

- [1] D. Gray & J. Le Kerneec, "Scan performance of small boat RCS enhancers," *IET Int radar conf.*, Chomping, China, 2023.
- [2] Ships and marine technology - marine radar reflectors - part 1: passive type, ISO 8729-1 1st ed., 2010-01-15.
- [3] D. Gray & J. Le Kerneec, "Development of an ISO8729 compliant passive RCS enhancer, part 1 - design of natural plastic lenses," *IEICE Tech. Rep.*, Sinfonia Hall, Ise, vol. 123, no. 378, AP2023-200, Feb. 2024.
- [4] O.J. Lodge & J.L. Howard, "On electric radiation and its concentration by lenses," *The London, Edinburgh, and Dublin Philosophical Magazine and Journal of Science*, vol. 28, iss. 170, pp. 48-65, 1889.
- [5] T. Maeda, S. Morisada, T. Kasajima & T. Hashida, "Elliptic wave-guide and method of fabricating it," *United States patent 3,546,916*, granted 15th December, 1970.
- [6] J.P. Watts & P.M. Hague, "Apparatus for propagating radio waves," *Great Britian patent 2,582,892*, granted 14th October, 2020.
- [7] M. Kilian & P. Kohl, "Asymetric waveguide," *European patent EP3,664,216*, granted 15th of November, 2023.
- [8] D.G. Bodnar, "Lens antennas," in *Antenna engineering handbook*, J.L. Volakis, Ed., New York: McGraw-Hill, 2007.